

Zig-zag dynamics in a Stern-Gerlach spin measurement

Simon Krekels^{*}, Christian Maes^{*}, Kasper Meerts^{*}, and Ward Struyve^{*,†}

^{*}Department of Physics and Astronomy, KU Leuven

[†]Centre for Logic and Philosophy of Science, KU Leuven

Abstract

The one-century-old Stern-Gerlach setup is paradigmatic for a quantum measurement. We visualize the electron trajectories following the Bohmian zig-zag dynamics. This dynamics was developed in order to deal with the fundamentally massless nature of particles (with mass emerging from the Brout-Englert-Higgs mechanism). The corresponding trajectories exhibit a stochastic zig-zagging, as the result of the coupling between left- and right-handed chiral Weyl states. This zig-zagging persists in the non-relativistic limit, which will be considered here, and which is described the Pauli equation for a nonuniform external magnetic field. Our results clarify the different meanings of “spin” as a property of the wave function and as a random variable in the Stern-Gerlach setup, and they illustrate the notion of effective collapse. We also examine the case of an EPR-pair. By letting one of the entangled particles pass through a Stern-Gerlach device, the nonlocal influence (action-at-a-distance) on the other particle is manifest in its trajectory, *e.g.* by initiating its zig-zagging.

Dedicated to the memory of Detlef Dürr, friend and mentor.

1 Introduction

Bohmian mechanics (also known as the de Broglie-Bohm or pilot-wave theory) describes the motion of point-particles guided by the wave function [1–3]. The nonrelativistic dynamics originally presented by de Broglie and Bohm is deterministic. The extension of this dynamics to quantum field theory proposed by Dürr *et al.* introduces a stochastic element [4–7]. More specifically, the events of particle creation and annihilation are stochastic, interrupting the otherwise deterministic motion. Furthermore, taking the particles to be fundamentally massless, as suggested by the Standard Model of particle physics, implies that even single fermions will evolve stochastically, with the motion alternatingly being determined by a left- and right-handed chiral Weyl spinor [8, 9]. The resulting particle dynamics exhibits a zig-zag like motion; the trajectories are continuous, but the velocities are not.¹ This type of motion is analogous to the run-and-tumble dynamics, which is well known for the description of, *e.g.*, self-propelling bacteria [11, 12].

For quite some time, the Bohmian trajectories have been studied and plotted in a variety of situations using the original deterministic Bohmian dynamics. The zig-zag dynamics on the other hand, has sofar received little attention. In a previous study, we considered the nonrelativistic limit of this dynamics in the case of the double-slit experiment [13]. Here, we continue that study in the context of another paradigmatic quantum measurement: the now centennial Stern-Gerlach experiment.

¹The Feynman diagrams display a similar zig-zag behavior [10, p. 630].

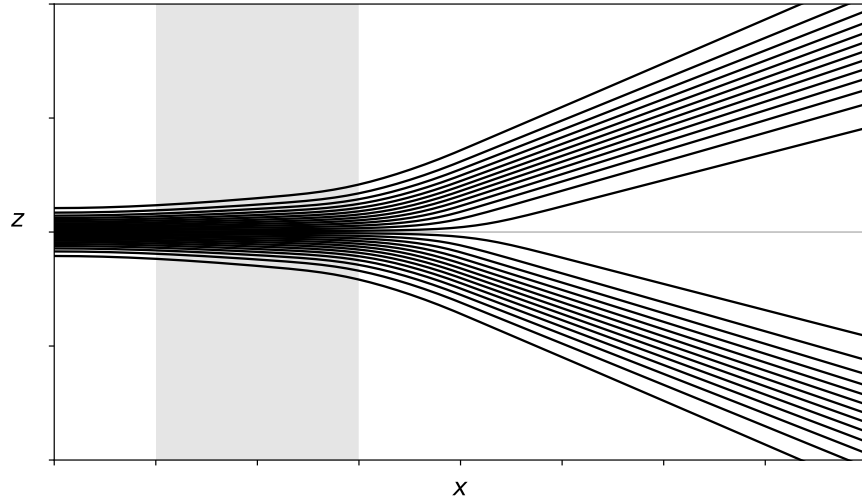


Figure 1: Some Bohmian trajectories for a Stern-Gerlach spin measurement in the z -direction, where the initial spinor has spin up in the y -direction (with the y -axis pointing into the plane of the paper, not drawn). The grey area indicates where the magnetic field is present.

There are several reasons to be interested in visualizing these trajectories. To start, there is the important fact that this is possible at all, despite earlier beliefs that a trajectory description of quantum systems must be fundamentally flawed. Secondly, it is helpful, much in the same sense that a trajectory-based description of Brownian motion through the Langevin equation is an essential methodological complement to its Fokker-Planck equation, which describes the evolution of densities. Furthermore, there are advantages related to specific questions and illustrations; for example, the making explicit of nonlocality, a fundamental feature of nature as shown by Bell, building on the work of Einstein, Podolsky and Rosen [14]. Or, as another example, the visualization of the formation of the interference pattern in double-slit experiments [13, 15–17].

In the present work, we concentrate on *measuring spin* which has its own history of confusion. While the Stern-Gerlach experiment is sometimes described as *the discovery of spin*, its initial history is more complicated. The original experiment of 1922 was motivated by disbelief on the part of Stern in the Bohr-Sommerfeld quantization of the direction of the angular momentum.

If this nonsense of Bohr should in the end prove to be right, we will quit physics!
— Oath sworn by Otto Stern and Max von Laue.

In other words, Stern wanted to test the hypothesis of directional quantization, as explicitly stated by Bohr (1913) in his atomic model, and as extended by Sommerfeld (1916). He found Gerlach ready for a “magnetic” experiment, and their experimental setup has been well-known ever since. In the original experiment, a narrow beam of silver atoms was shot through a region with a nonuniform magnetic field. Upon leaving the magnetic field, the atoms hit a detection screen and the beam was observed to be split in two. The classical prediction would be a continuous distribution, as for randomly oriented magnetic dipoles. Pauli wrote to Gerlach, “This should convert even the nonbeliever Stern.”. The Stern-Gerlach publication [18] was given the title “Experimental evidence of directional quantization in a magnetic field.”

However, as a matter of fact, silver has no orbital angular momentum; what Stern and Gerlach measured was *spin*, an intrinsic form of angular momentum. It was Kronig in 1925 who proposed

electron spin, yet never published his proposal. After finding the idea “quite ridiculous”, Pauli wrote about “a classically non-describable two-valuedness” [19]. A few months later, Uhlenbeck and Goudsmit used these ideas to convincingly explain the Zeeman effect [20, 21], and in that way, they were the first to explicitly introduce electron spin. See [22, 23] for more history and references.

The main aim of the present paper is to visualize the influence of spin (coupled to an inhomogeneous magnetic field) on the motion of electrons in the Stern-Gerlach setup. That problem has been treated before with the standard Bohmian dynamics [24–29], to generate trajectories as displayed in Fig. 1. Here, we consider the zig-zag dynamics in the nonrelativistic limit, with the Pauli equation as governing wave equation.

While visualizing these dynamics, we also learn something about spin in the context of so-called hidden variable theories. The confusion perhaps starts with the word *spin* being used in various ways, and having various meanings. We say that the electron has spin 1/2, which means that its wave function is a spinor. Another thing is to *measure spin* in a particular direction, with outcomes that can be *up* or *down*. The word “measurement” then suggests that the experiment reveals some pre-determined value for the spin, but as we will see (and as is well-known in Bohmian mechanics), this is not the case. Instead, the spin is co-determined by the system and the details of the experimental setup (a property called *contextuality* [29–31]).

In Section 2, we introduce the Bohmian evolution equations for an electron in an electromagnetic field. We then apply these equations to a Stern-Gerlach type setup in Section 3. We consider an entangled 2-electron system in Section 4 and compare the situation where both particles are evolving freely with the situation where one of the electrons is sent through a Stern-Gerlach device. There we visualize how this affects the zig-zagging of the other electron as an *action-at-a-distance*.

2 Zig-zag dynamics

In the nonrelativistic limit [9], the zigzag dynamics for a single electron describes the change of its position \mathbf{X} and chirality $\chi = \pm 1$ by

$$\dot{\mathbf{X}}(t) = \mathbf{v}_{\chi(t)}(\mathbf{X}(t), t), \quad \chi(t) \rightarrow -\chi(t) \text{ at rate } r_{-\chi(t)}(\mathbf{X}(t), t), \quad (1)$$

where the velocity $\mathbf{v}_{\chi}(\mathbf{x}, t)$ and jump rate $r_{\chi}(\mathbf{x}, t)$ are determined by the Pauli spinor $\Psi(\mathbf{x}, t)$ as follows,

$$\mathbf{v}_{\chi} = \frac{\hbar}{m} \frac{\text{Im}(\Psi^{\dagger} \mathbf{D} \Psi)}{\Psi^{\dagger} \Psi} + \frac{\hbar}{2m} \frac{\nabla \times (\Psi^{\dagger} \boldsymbol{\sigma} \Psi)}{\Psi^{\dagger} \Psi} + c \chi \mathbf{s} \quad (2)$$

$$r_{\chi} = \left[c \chi \frac{\nabla \cdot (\Psi^{\dagger} \boldsymbol{\sigma} \Psi)}{\Psi^{\dagger} \Psi} \right]^+ = \left[2c \chi \frac{\text{Re} \Psi^{\dagger} \boldsymbol{\sigma} \cdot \nabla \Psi}{\Psi^{\dagger} \Psi} \right]^+, \quad F^+ = \max(F, 0), \quad (3)$$

where $\mathbf{D} = \nabla - ie\mathbf{A}/\hbar c$ is the covariant derivative with vector potential \mathbf{A} , and

$$\mathbf{s} = \frac{\Psi^{\dagger} \boldsymbol{\sigma} \Psi}{\Psi^{\dagger} \Psi}, \quad (4)$$

with $\boldsymbol{\sigma}$ the vector of the three Pauli matrices, is the spin vector. The Pauli spinor satisfies the Pauli equation, which in an external electromagnetic potential (V, \mathbf{A}) with corresponding magnetic field \mathbf{B} , reads

$$i\hbar \partial_t \Psi = -\frac{\hbar^2}{2m} \mathbf{D}^2 \Psi - \frac{e\hbar}{2mc} \mathbf{B} \cdot \boldsymbol{\sigma} \Psi + eV \Psi. \quad (5)$$

The Fokker-Planck equation associated to the stochastic dynamics (1) is

$$\partial_t \rho(\mathbf{x}, \chi, t) + \nabla \cdot (\mathbf{v}_\chi \rho(\mathbf{x}, \chi, t)) = r_\chi \rho(\mathbf{x}, -\chi, t) - r_{-\chi} \rho(\mathbf{x}, \chi, t). \quad (6)$$

A particular solution is given by $\rho(\mathbf{x}, \chi, t) = \Psi^\dagger \Psi / 2$, since the Pauli equation (5) implies

$$\partial_t(\Psi^\dagger \Psi) + \nabla \cdot (\mathbf{v}_\chi \Psi^\dagger \Psi) = r_\chi \Psi^\dagger \Psi - r_{-\chi} \Psi^\dagger \Psi. \quad (7)$$

Therefore, the dynamics (1) preserves the *quantum equilibrium distribution* $\Psi^\dagger \Psi$, which is important in establishing the usual quantum predictions determined by the Born rule [3, 32]. (In the relativistic case, the equilibrium distribution $\rho^{\psi_\pm}(\mathbf{x}, \pm 1, t)$ is determined by the right- and left-handed Weyl spinor ψ_\pm and hence the right- and left-handed part are generically different. In the nonrelativistic limit, the chiral components become equal, at least to the lowest order.)

Note that (1) is a Langevin-type equation, and may be recognized as describing run-and-tumble dynamics, with the spacetime profile of the Pauli spinor playing the role chemotaxis does for run-and-tumble bacteria [13]. The Fokker-Planck equation for the density of two-state run-and-tumble particles is precisely (6).

The chirality jumps generate the zig-zag motion of the particles. The chirality dependence of the velocity \mathbf{v}_χ is only in the third term of (2), which is proportional to the spin vector. This term is also the dominating contribution to the velocity since its norm is given by the light speed c . As a consequence, the particle travels approximately at the speed of light and approximately in the direction of the spin vector. (In the relativistic case, the velocity is *exactly* along the direction of the spin vector corresponding to the left- or right-handed Weyl spinor and the motion is always luminal [9].)

In earlier formulations of a Bohmian dynamics for the Pauli theory, there was no stochasticity. In the simplest formulation, the velocity of the particle is given by only the first term of (2) [1, 2]. The second term was motivated by considering the nonrelativistic limit of the Bohmian dynamics for the Dirac theory [1]. There are already striking differences resulting from the addition of this second term, for example in hydrogenic atoms [33] and in the double slit experiment [16]. The inclusion of the third term and the jumps entails further significant changes, as illustrated in [13] for the double-slit experiment. One immediate consequence is that the particle can never be at rest, unlike those earlier formulations where the particle remains at rest for certain energy eigenstates (which was a feature that bothered Einstein [34, 35]).

For a multiple-electron system, the Pauli equation for $\Psi(\mathbf{x}_1, \dots, \mathbf{x}_N, t)$ is

$$i\hbar \partial_t \Psi = \sum_{k=1}^N \left[-\frac{\hbar^2}{2m} \mathbf{D}_k^2 \Psi - \frac{e\hbar}{2mc} \mathbf{B}(\mathbf{x}_k) \cdot \boldsymbol{\sigma}_k \Psi + eV(\mathbf{x}_k) \Psi \right], \quad (8)$$

where now $\mathbf{D}_k = \nabla_k - ie\mathbf{A}(\mathbf{x}_k)/\hbar c$. The corresponding zig-zag dynamics for the k th particle is

$$\dot{\mathbf{X}}_k(t) = \mathbf{v}_{k, \chi_k(t)}(\mathbf{X}_1(t), \dots, \mathbf{X}_N(t), t), \quad (9)$$

with

$$\mathbf{v}_{k, \chi_k} = \frac{\hbar}{m} \frac{\text{Im}(\Psi^\dagger \mathbf{D}_k \Psi)}{\Psi^\dagger \Psi} + \frac{\hbar}{2m} \frac{\nabla_k \times (\Psi^\dagger \boldsymbol{\sigma}_k \Psi)}{\Psi^\dagger \Psi} + c\chi_k \mathbf{s}_k, \quad (10)$$

where $\boldsymbol{\sigma}_k = I \otimes \dots \otimes I \otimes \boldsymbol{\sigma} \otimes I \otimes \dots \otimes I$, with $\boldsymbol{\sigma}$ at the k -th of the N places, and

$$\mathbf{s}_k = \frac{\Psi^\dagger \boldsymbol{\sigma}_k \Psi}{\Psi^\dagger \Psi} \quad (11)$$

is the spin vector for the k th particle. The jump rate for one of the chiralities, say the k th, to flip from $-\chi_k$ to χ_k at time t is given by

$$r_{k,\chi_k}(\mathbf{X}_1(t), \dots, \mathbf{X}_N(t), t), \quad (12)$$

with

$$r_{k,\chi_k} = \left[c\chi_k \frac{\nabla_k \cdot (\Psi^\dagger \boldsymbol{\sigma}_k \Psi)}{\Psi^\dagger \Psi} \right]^+. \quad (13)$$

It is crucial here that \mathbf{v}_{k,χ_k} and r_{k,χ_k} depend on the full wave function (multi-particle spinor Ψ), which implies that the dynamics of one particle may nonlocally depend on the motion of the other particles. In particular, the spin vector and hence the (approximate) direction of zig-zagging may depend on the whole configuration.

Unlike the single-particle case, the velocity need not be luminal (which is also true in the full relativistic theory). This is because for an entangled spinor, the norm of the spin vector \mathbf{s}_k may be smaller than one. We will encounter examples in Section 4.

3 Stern-Gerlach setup

3.1 Solution of Pauli equation

In the Stern-Gerlach setup, a beam of separate spinful particles is sent through an inhomogeneous magnetic field, resulting in a splitting of the beam and two detection bands on a final detecting screen. Nonrelativistically, such particles are described by the Pauli equation (5), which in natural units $\hbar = m = c = 1$, is given by

$$i\partial_t \Psi = -\frac{1}{2} \nabla^2 \Psi - \frac{e}{2} \mathbf{B} \cdot \boldsymbol{\sigma} \Psi, \quad (14)$$

where the magnetic field is nonzero only between some initial and final time t_i and t_f , *i.e.*,

$$\mathbf{B}(t) = \begin{cases} (0, 0, 0) & \text{if } t < t_i, \\ (0, 0, 2bz/e) & \text{if } t_i < t < t_f, \\ (0, 0, 0) & \text{if } t > t_f. \end{cases} \quad (15)$$

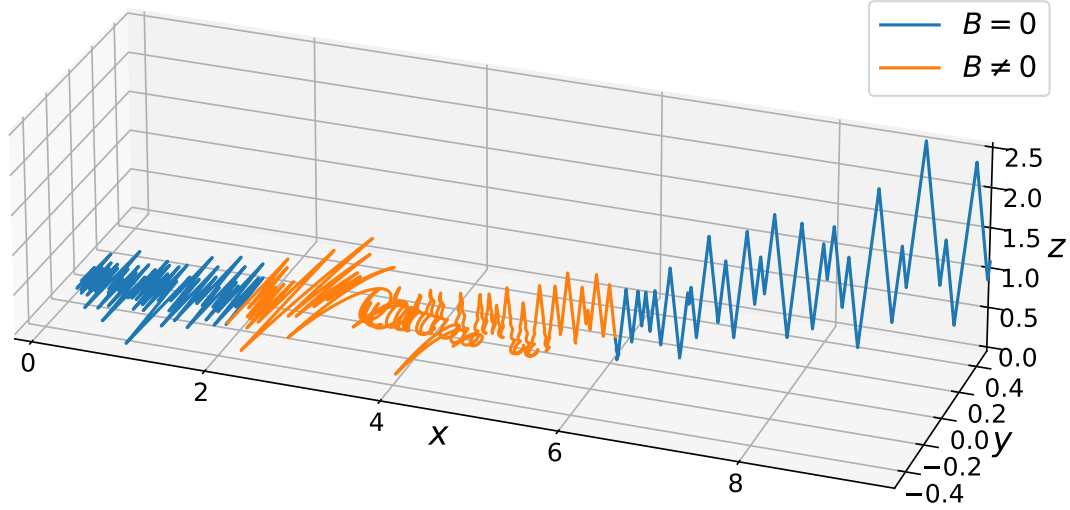
Note that, for convenience, the magnetic field is taken to be time-dependent, and not space-dependent as in the original Stern-Gerlach setup. The magnetic field will be taken nonzero when the bulk of the packet passes through the region of the Stern-Gerlach magnets. We have also adopted the usual approximations where the vector potential is dropped in the kinetic term and the magnetic field does not satisfy Maxwell's equations, since $\nabla \cdot \mathbf{B} \neq 0$ (see *e.g.* [36, pp. 328-330] for further discussion). The goal is to provide a qualitatively correct and clear picture, and these approximations allow us to do precisely that, as (14) allows for an analytic solution [37].

Consider an initial Pauli spinor

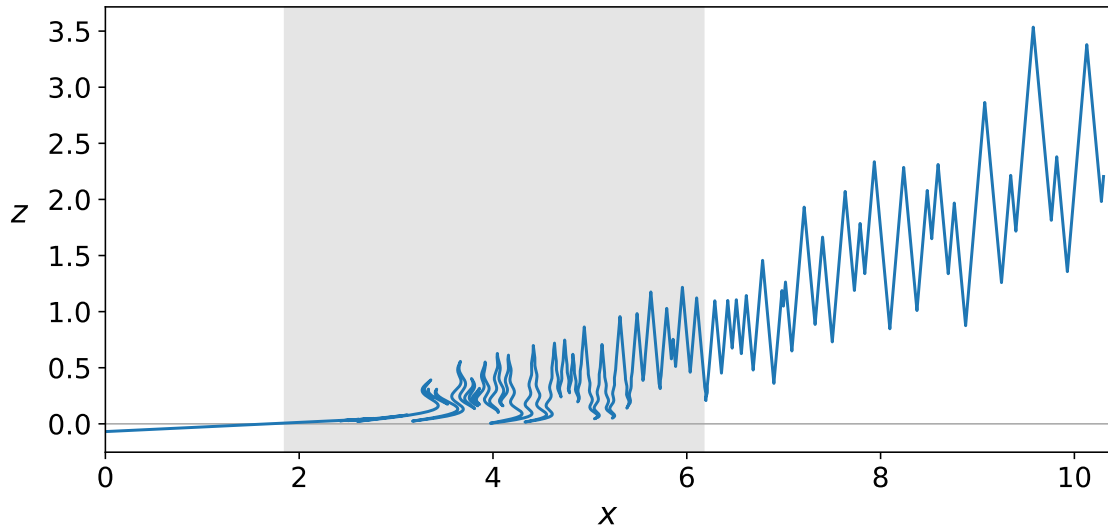
$$\Psi(\mathbf{x}, 0) = \psi(\mathbf{x}, 0) \begin{pmatrix} c_+ \\ c_- \end{pmatrix}, \quad (16)$$

with $c_\pm \in \mathbb{C}$, and where the scalar wave function

$$\psi(\mathbf{x}, 0) = \psi_x(x, 0)\psi_y(y, 0)\psi_z(z, 0) \quad (17)$$



(a)



(b)

Figure 2: Particle trajectory for the spinor $\Psi = \frac{1}{\sqrt{2}}(\psi_+, i\psi_-)^T$, which has initial spin *up* in the *y*-direction. Fig. 2b shows the *xz*-projection of Fig. 2a. The area where the magnetic field is turned on is marked by a different line colour and a grey background in Figs. 2a & 2b respectively. As is clear from the figure, the particle may cross the *xy*-plane.

is Gaussian with momentum p in the x -direction, and has widths d_x, d_y, d_z in the various directions, *i.e.*,

$$\psi_x(x, 0) = \frac{1}{(2\pi d_x^2)^{1/4}} \exp\left(-\frac{x^2}{4d_x^2} + ipx\right), \quad (18)$$

$$\psi_y(y, 0) = \frac{1}{(2\pi d_y^2)^{1/4}} \exp\left(-\frac{y^2}{4d_y^2}\right), \quad \psi_z(z, 0) = \frac{1}{(2\pi d_z^2)^{1/4}} \exp\left(-\frac{z^2}{4d_z^2}\right).$$

Using the propagator found in [37], the solution of (14) is

$$\Psi(\mathbf{x}, t) = \begin{pmatrix} c_+ \psi_+(\mathbf{x}, t) \\ c_- \psi_-(\mathbf{x}, t) \end{pmatrix}, \quad (19)$$

where

$$\psi_{\pm}(\mathbf{x}, t) = \psi_x(x, t) \psi_y(y, t) \psi_{z, \pm}(z, t), \quad (20)$$

with

$$\begin{aligned} \psi_x(x, t) &= \frac{1}{\left[2\pi d_x^2 \left(1 + \frac{it}{2d_x^2}\right)^2\right]^{1/4}} \exp\left[-\frac{(x - pt)^2}{4d_x^2 \left(1 + \frac{it}{2d_x^2}\right)} + ipx - i\frac{p^2}{2}t\right], \\ \psi_y(y, t) &= \frac{1}{\left[2\pi d_y^2 \left(1 + \frac{it}{2d_y^2}\right)^2\right]^{1/4}} \exp\left[-\frac{y^2}{4d_y^2 \left(1 + \frac{it}{2d_y^2}\right)}\right], \\ \psi_{z, \pm}(z, t) &= \frac{1}{\left[2\pi d_z^2 \left(1 + \frac{it}{2d_z^2}\right)^2\right]^{1/4}} \\ &\quad \times \begin{cases} \exp\left[-\frac{z^2}{4d_z^2 \left(1 + \frac{it}{2d_z^2}\right)}\right] & \text{if } t < t_i \\ \exp\left[-\frac{\left(z \mp \frac{b(t-t_i)^2}{2}\right)^2}{4d_z^2 \left(1 + \frac{it}{2d_z^2}\right)} \pm ib(t-t_i)z - i\frac{b^2(t-t_i)^3}{6}\right] & \text{if } t_i < t < t_f \\ \exp\left[-\frac{\left(z \mp \frac{b(t_f-t_i)^2}{2} \pm b(t_f-t_i)(t-t_f)\right)^2}{4d_z^2 \left(1 + \frac{it}{2d_z^2}\right)} \right. \\ \quad \left. \pm ib(t_f-t_i)z - i\frac{b^2(t_f-t_i)^3}{6} - i\frac{b^2(t_f-t_i)^2}{2}(t-t_f)\right] & \text{if } t_f < t \end{cases}. \end{aligned} \quad (21)$$

3.2 Integrating the zig-zag dynamics

To numerically integrate the trajectories corresponding to the wave function (21), we make use of the code developed for our previous study [13] (extending it to allow for wave functions that are not spin eigenstates).

The propagation of the particle consists of two parts. First, the velocity field (10) is a first-order ordinary differential equation, for which we employ the Cash-Karp method, a Runge-Kutta method

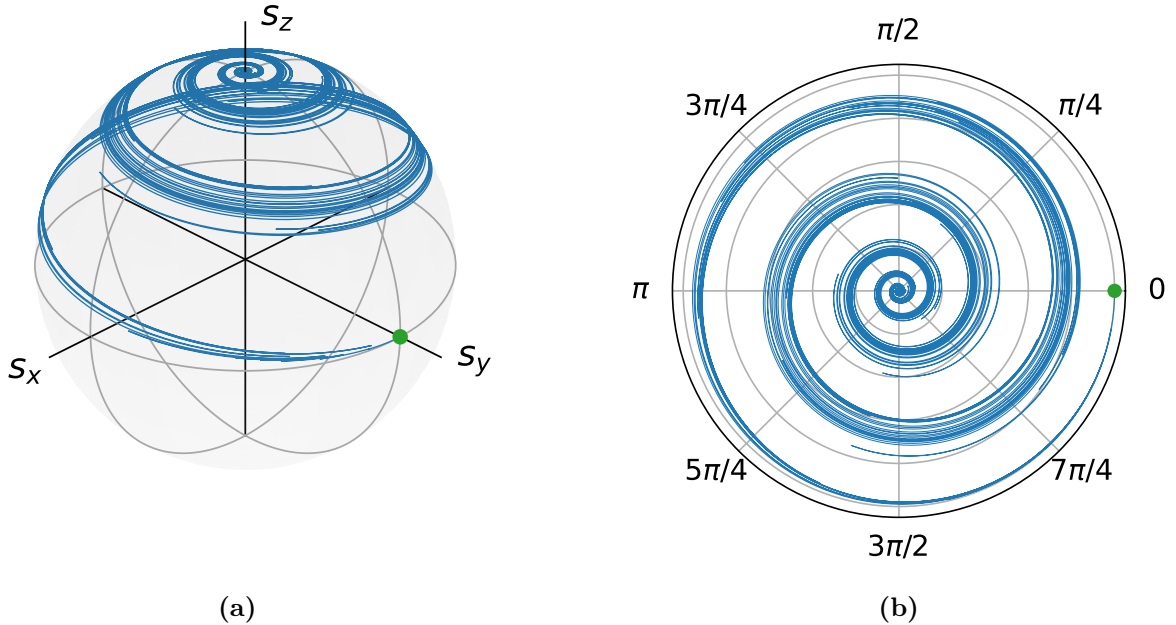


Figure 3: Spin vector along the trajectory plotted in Fig. 2. Fig. 3a shows the 3D evolution of the spin vector on the unit sphere, which can be identified with the Bloch sphere, while Fig. 3b shows its projection onto the xy -plane. It shows the transitioning of the spin vector from the positive y -direction to the positive z -direction. The winding up and down the sphere is a direct consequence of the particle zigzagging back and forth in position space, where the spin vector varies spatially, cf. Fig. 4.

which yields a fifth-order accurate solution, as well as a fourth-order estimate for the error. This estimate is then used to adaptively adjust the time step to keep the local truncation error low, for which we set an absolute tolerance of 10^{-10} . At this point, we also make sure that the product of the tumbling rate and the time step remains reasonably low, below 2^{-7} . This product is then taken to be the probability for the particle to undergo a chirality jump during this time step. This integration step is repeated until the final time is reached. See [38] for the publicly available code.

The parameters chosen to integrate the dynamics (1) using the solution (19) are $d_x = d_y = d_z = 100$, $b = 10^{-6}$, and $p = 1/10$. The total running time is $T = 10^5$ and the magnetic field is turned on between $t_i = T/5$ and $t_f = 3T/5$. The space and time coordinates in all the figures have been rescaled with a factor of 10^3 to reduce visual clutter on the axes.

In Fig. 2, a trajectory is plotted for a spinor that initially has spin up in the y -direction, *i.e.*, $\Psi = \frac{1}{\sqrt{2}}(\psi_+, i\psi_-)^T$, so that $c_+ = 1/\sqrt{2}$ and $c_- = i/\sqrt{2}$. The spin vector \mathbf{s} along this trajectory is plotted in Fig. 3. As explained before, the zig-zagging happens approximately along the direction of the spin vector. From Fig. 2 it is clear that the zig-zagging which is initially along the y -direction transitions into a zig-zagging along the z -direction as it passes the magnetic field. As shown in Fig. 3, this transition involves some heavy oscillation (due to the jumps) before settling in the z -direction. This happens quite fast, with changes occurring only while the particle moves through the magnetic field.

The spin vector at time $t = 70$ (just after turning off the magnetic field) is plotted in Fig. 4. In

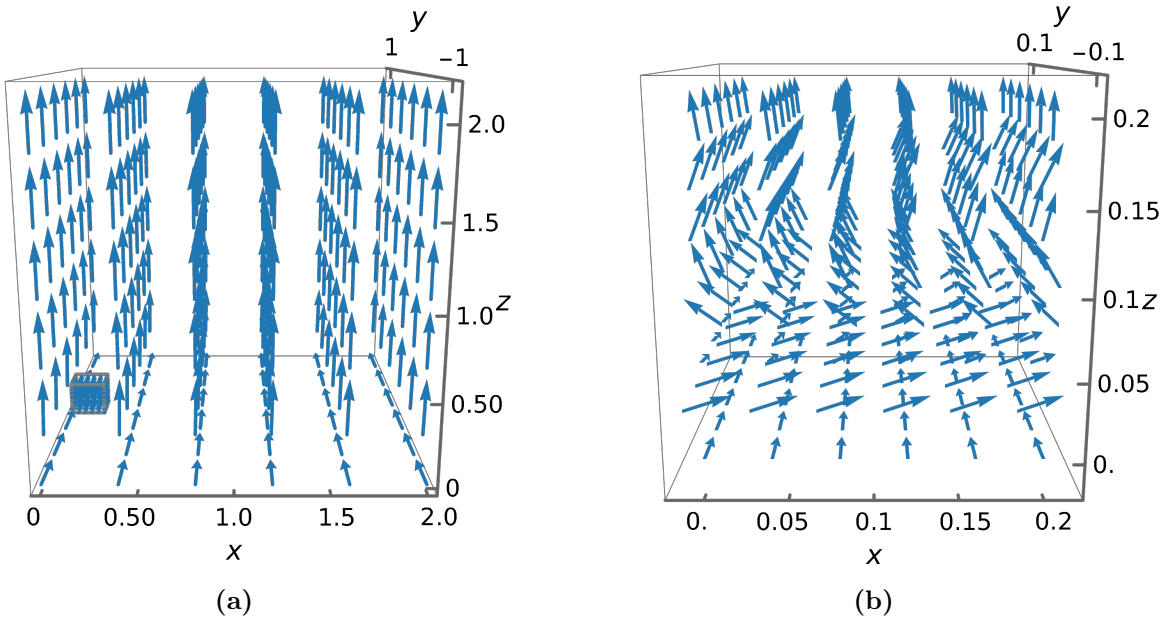


Figure 4: The spin vector above the xy plane ($z \geq 0$), at $t = 70$, just after turning off the magnetic field, for the spinor $\Psi = \frac{1}{\sqrt{2}}(\psi_+, i\psi_-)^T$, as in Figs. 2 and 3. Fig. 4b zooms in on part of Fig. 4a shown in the bottom left corner. Away from the xy -plane, the spin vector points in the positive z -direction, but near the plane it displays irregular behaviour, cf. Fig 3.

the region sufficiently above (below) the xy -plane the spin vector points in the positive (negative) z -direction. Near the xy -plane the spin vector shows more irregular behaviour, which explains the strong oscillation of the spin vector along the trajectory shown in Fig. 3. On the xy -plane, the spin vector points in the positive y -direction. So once the particle comes near this plane it will approximately start moving and zig-zagging along the y -direction.

Whenever the particle moves away from the bulk of the wave packet, the jump rate increases, increasing the probability that it changes chirality, and thus direction, and moves back towards the center of the packet. This is clear from Fig. 5 where the jump rates are plotted. So when a particle is above the xy -plane and moving down towards it, the probability for a jump increases, and with it, the probability to move back up. If no jump occurs and the particle gets near the xy -plane it will start moving approximately in the y -direction, where again the probability for a jump will increase when the particle moves further away from the bulk of the packet. Once the jump occurs, it will reverse its motion and will start moving up again eventually. While a particle may cross the xy -plane the probability for this to happen decreases over time, because of the separation of the packets ψ_+ and ψ_- .

Depending on the initial position and the jumps that took place, the final position ends up either above or below the xy -plane, which determines the outcome of the spin measurement by the Stern-Gerlach device.

The trajectory is markedly different from those in Fig. 1, which follow the original Bohmian dynamics for the same spinor.

In Fig. 6, 10 trajectories are plotted, with initial positions randomly drawn with a $\Psi^\dagger\Psi$ distri-

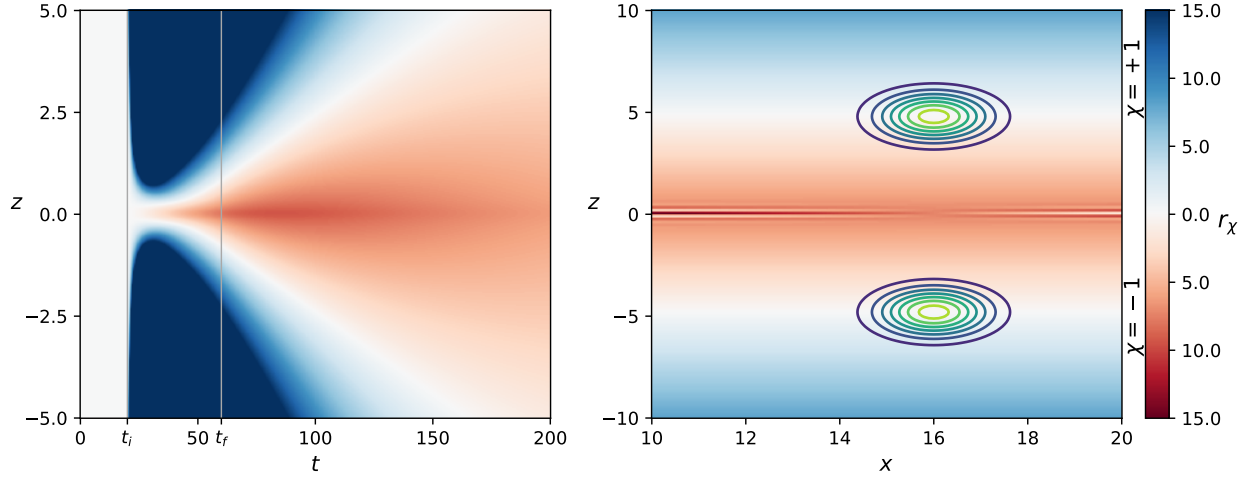


Figure 5: Left: Time-dependent tumbling rates for the spinor $\Psi = \frac{1}{\sqrt{2}}(\psi_+, i\psi_-)^\top$ as a function of z at $y = 0$ with the x -coordinate at the centre of the wave packet. Right: Tumbling rates at time 160, at $y = 0$. The contour lines connect equal densities $\Psi^\dagger \Psi(x, 0, z, 160)$.

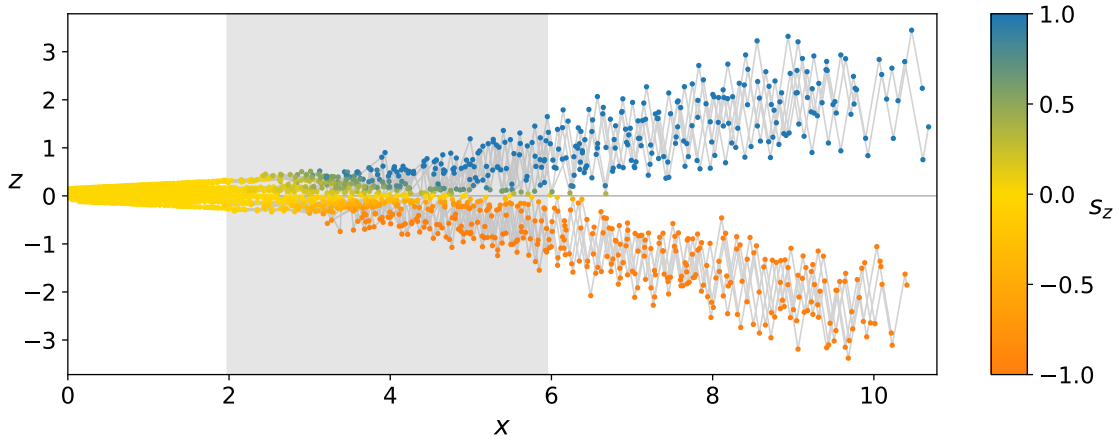


Figure 6: 10 particle trajectories for the spinor $\Psi = \frac{1}{\sqrt{2}}(\psi_+, i\psi_-)^\top$. The dots represent the locations of the particles at the times of jumps. The color of a dot indicates s_z , the z -component of the spin vector, at the jump event.

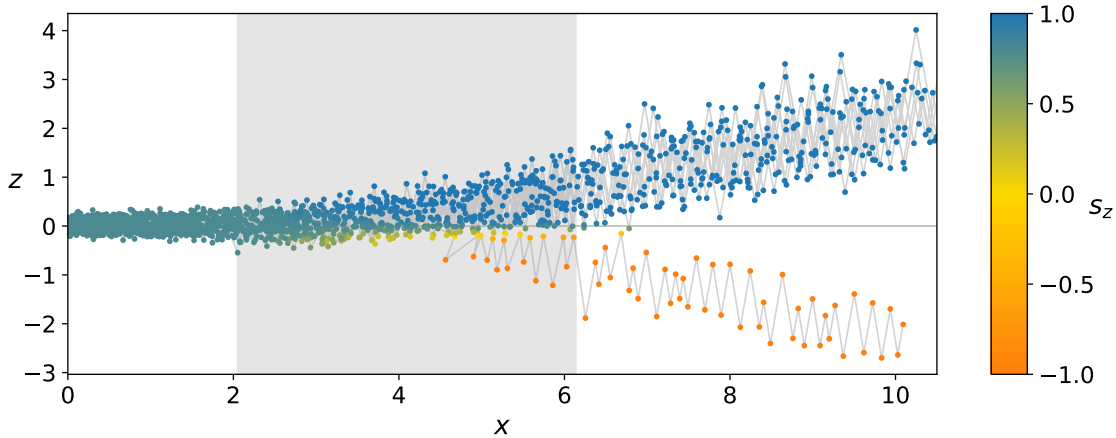


Figure 7: Ten particle trajectories for the spinor $\Psi = \frac{1}{\sqrt{10}}(3\psi_+, i\psi_-)^\top$. As in Fig. 6, the dots represent the locations of the particles at the times of jumps. The color of a dot indicates s_z at the jump event.

bution, again for the state $\Psi = \frac{1}{\sqrt{2}}(\psi_+, i\psi_-)^\top$, which has initial spin along the y-direction. The locations where jumps occur are represented by a dot. The color of the dot represents the value of s_z , the z-component of the spin vector, at those locations, at the time of the chirality flip.

In Fig. 7, similarly, trajectories are plotted for the wave function $\Psi = \frac{1}{\sqrt{10}}(3\psi_+, i\psi_-)^\top$. In this case, the initial spin vector is $(0, 6/10, 8/10)$. More trajectories end up in the upper beam. This reflects the usual quantum probability of 9/10 for the particle to be found with spin *up* in the z-direction. The chirality jumps play a role in deciding whether the particle ends up with a positive or negative z-coordinate.

As mentioned before, the separation of the waves ψ_+ and ψ_- , which happens after passage through the magnets, implies that the particle tends to stay within the bulk of either the wave ψ_+ or ψ_- and does not tend to move between ψ_+ and ψ_- .² This also implies an *effective collapse*. Namely, if the particle goes in the positive z-direction after passing the magnets, its dynamics is effectively determined only by ψ_+ (since the velocity and the jump rate only depend on the wave function in the neighborhood of the particle). This means that (as long as the support of ψ_+ and ψ_- remain disjoint, and the particle does not cross the xy -plane), the ψ_- part can be ignored in the description of the particle, amounting to an effective collapse of the spinor to $(\psi_+, 0)^\top$.³

Note that for a given identical realization of the trajectory, but with an inverted magnetic field, the observed spin would be opposite [40, p. 153], [29]. Therefore, the observed spin value is not only determined by the state of the system (particle position and wave function), but also by how the experiment is performed. This is an instance of *contextuality* [30, 31].

²The fact that the particle does not tend to move between supports of non-overlapping wave functions, will even be amplified for macroscopic objects. So, in particular, this will imply stability of macroscopic records, which is important in showing that the theory is empirically adequate [32].

³There is actually a more precise notion of collapse in Bohmian mechanics. This requires the notion of the wave function of a subsystem, which can be naturally defined in terms of the wave function of the universe and the particle positions of the environment [32]. In the present case, which deals with spin, the state of a subsystem is a density matrix, called the *conditional density matrix*, rather than a wave function, and this density matrix will actually collapse in measurement situations [39].

We summarize the main features: the outcome of the spin measurement depends on where the particle ends up after passing through the Stern-Gerlach device. Where it ends up depends not only on the initial position but also on the jumps that have occurred. Furthermore, if at $t = 0$ the particle position has distribution $\Psi^\dagger(\mathbf{x}, 0)\Psi(\mathbf{x}, 0)$, then at time t it has distribution $\Psi^\dagger(\mathbf{x}, t)\Psi(\mathbf{x}, t)$, in accordance with the Born rule.

4 Stern-Gerlach with a pair of entangled particles

When there are no electromagnetic potentials, a particular solution of the 2-particle Pauli equation (8) is given by the entangled spinor

$$\Psi(\mathbf{x}_1, \mathbf{x}_2, t) = \psi_1(\mathbf{x}_1, t)\psi_2(\mathbf{x}_2, t) \left[a \begin{pmatrix} 1 \\ 0 \end{pmatrix} \begin{pmatrix} 0 \\ 1 \end{pmatrix} - b \begin{pmatrix} 0 \\ 1 \end{pmatrix} \begin{pmatrix} 1 \\ 0 \end{pmatrix} \right], \quad (22)$$

where a and b are real constants, and where ψ_1 and ψ_2 are scalar wave functions for particles 1 and 2 respectively, satisfying the free Schrödinger equation. We have that

$$\Psi^\dagger \boldsymbol{\sigma}_1 \Psi = |\psi_1|^2 |\psi_2|^2 (a^2 - b^2) \mathbf{e}_z = -\Psi^\dagger \boldsymbol{\sigma}_2 \Psi. \quad (23)$$

So the spin vectors of the two particles will always be pointing in opposite directions. In addition, the velocity fields (10) for the two particles reduce to

$$\mathbf{v}_{k, \chi_k} = \frac{\hbar}{m} \frac{\text{Im}(\psi_k^* \nabla_k \psi_k)}{|\psi_k|^2} - (-1)^k \frac{a^2 - b^2}{a^2 + b^2} \left[\frac{\hbar}{2m} \nabla_k \times (\ln |\psi_k|^2 \mathbf{e}_z) + c\chi_k \right], \quad k = 1, 2, \quad (24)$$

and the jump rates (13) become

$$r_{\chi_k} = \left[-c\chi_k (-1)^k \frac{a^2 - b^2}{a^2 + b^2} \partial_{z_k} \ln |\psi_k|^2 \right]^+, \quad k = 1, 2. \quad (25)$$

As such, the spin-dependent part in both the velocity and the jump rates decreases when a approaches b . In the special case that $a = b$, the spin-dependent part completely vanishes,⁴ so that the dynamics becomes

$$\dot{\mathbf{X}}_k = \frac{\hbar}{m} \frac{\text{Im}(\psi_k^* \nabla_k \psi_k)}{|\psi_k|^2}. \quad (26)$$

That is, the dynamics amounts to the original one introduced by de Broglie and Bohm, and the particles also move entirely independently.

As a particular example of the case where $a = b$, we can consider ψ_1 and ψ_2 to be Gaussians initially localized at the origin which are moving away from each other. That is, we take particle 1 with positive momentum p and particle 2 with negative momentum $-p$ along the x -axis. Denoting the solution (19) by

$$\Psi_{p, \mathbf{B}}(\mathbf{x}, t) = \frac{1}{\sqrt{2}} \begin{pmatrix} \psi_{p, \mathbf{B}, +}(\mathbf{x}, t) \\ \psi_{p, \mathbf{B}, -}(\mathbf{x}, t) \end{pmatrix}, \quad (27)$$

the spinor corresponding to the two particles moving freely apart ($\mathbf{B} = \mathbf{0}$) is

$$\Psi_{\text{free}}(\mathbf{x}_1, \mathbf{x}_2, t) = \frac{1}{\sqrt{2}} \psi_{p, \mathbf{0}, +}(\mathbf{x}_1, t) \psi_{-p, \mathbf{0}, +}(\mathbf{x}_2, t) \left[\begin{pmatrix} 1 \\ 0 \end{pmatrix} \begin{pmatrix} 0 \\ 1 \end{pmatrix} - \begin{pmatrix} 0 \\ 1 \end{pmatrix} \begin{pmatrix} 1 \\ 0 \end{pmatrix} \right], \quad (28)$$

⁴For a single particle, this is impossible since its spin vector (4) has norm one and never vanishes.

where $\psi_{p,\mathbf{0},+} = \psi_{p,\mathbf{0},-}$. For this state, the particle dynamics is of the form (26), without the zig-zagging.

Let us now compare this to the case where particle 1 is sent through a Stern-Gerlach device. In this case, the spinor is

$$\Psi_{\text{SG}}(\mathbf{x}_1, \mathbf{x}_2, t) = \psi_{-p,\mathbf{0},+}(\mathbf{x}_2, t) \left[\psi_{p,\mathbf{B},+}(\mathbf{x}_1, t) \begin{pmatrix} 1 \\ 0 \end{pmatrix} \begin{pmatrix} 0 \\ 1 \end{pmatrix} - \psi_{p,\mathbf{B},-}(\mathbf{x}_1, t) \begin{pmatrix} 0 \\ 1 \end{pmatrix} \begin{pmatrix} 1 \\ 0 \end{pmatrix} \right]. \quad (29)$$

The spin vectors remain opposite, *i.e.*,

$$\mathbf{s}_1(\mathbf{x}_1, \mathbf{x}_2, t) = -\mathbf{s}_2(\mathbf{x}_1, \mathbf{x}_2, t) = \frac{|\psi_{p,\mathbf{B},+}(\mathbf{x}_1, t)|^2 - |\psi_{p,\mathbf{B},-}(\mathbf{x}_1, t)|^2}{|\psi_{p,\mathbf{B},+}(\mathbf{x}_1, t)|^2 + |\psi_{p,\mathbf{B},-}(\mathbf{x}_1, t)|^2} \mathbf{e}_z. \quad (30)$$

Note that the spin vectors only depend on \mathbf{x}_1 , so their value along a trajectory only depends on the position of particle 1. Their direction is always along the z -axis. The spin vector \mathbf{s}_1 will be pointing along the positive (negative) z -axis if the z -coordinate of particle 1 is greater (smaller) than zero. Initially, at time $t = 0$, the spin vectors are zero. The magnetic field causes a separation of the wave functions $\psi_{p,\mathbf{B},+}$ and $\psi_{p,\mathbf{B},-}$, causing the spin vector of both particles to become nonzero. As is shown in Figs. 8–9, once particle 1 enters the Stern-Gerlach device it starts zig-zagging and this causes particle 2 to also start zig-zagging. While particle 1 goes up in the z -direction, thereby displaying the result of the spin measurement, particle 2 keeps zig-zagging around $z = 0$. Other trajectories display similar behavior, with particle 1 ending up either *up* or *down*, depending on the initial position and the jumps.

After passage through the magnetic field, there is an effective collapse of Ψ_{SG} . In the present case, this is to

$$\psi_{-p,\mathbf{0},+}(\mathbf{x}_2, t) \psi_{p,\mathbf{B},+}(\mathbf{x}_1, t) \begin{pmatrix} 1 \\ 0 \end{pmatrix} \begin{pmatrix} 0 \\ 1 \end{pmatrix}, \quad (31)$$

which is a product wave function. So the dynamics of particle 1 is determined by $\psi_{p,\mathbf{B},+}(\mathbf{x}_1, t)(1, 0)^\top$, while that of particle 2 is determined by $\psi_{-p,\mathbf{0},+}(\mathbf{x}_2, t)(0, 1)^\top$. If a spin measurement in the z -direction were to be performed on particle 2, it would yield the result spin *down*, in agreement with the Born rule which predicts perfect anti-correlation of the spin measurement results.

If the Stern-Gerlach device were rotated in the y -direction, both particles would end up zig-zagging in that direction (since the initial spinor is rotationally invariant). So whether particle 1 is moving through a Stern-Gerlach device or not, as well as the direction of the corresponding magnetic field, have an effect on particle 2. This effect is instantaneous and is an instance of nonlocality. (That was also illustrated for the dynamics without the zig-zagging in [26, 27, 29].)

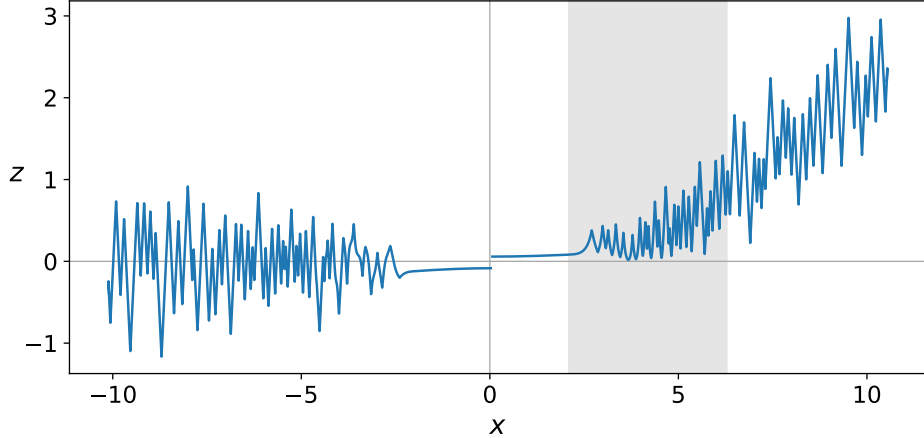


Figure 8: A set of trajectories for the entangled spinor Ψ_{SG} given in (29), projected in the xz -plane. Initially, the particles are moving without zig-zagging. The zig-zagging of both particles starts once particle 1 enters the Stern-Gerlach device. After passing through the device the zig-zagging is along the z -direction for both particles.

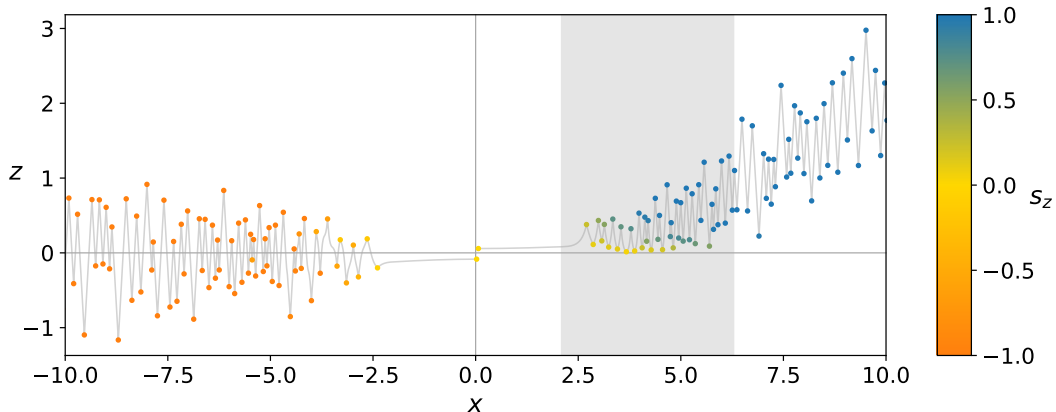


Figure 9: The same trajectories as in Fig. 8, with dots at the location of the chirality jumps and the color indicating the value of s_z .

5 Conclusions

Textbooks in quantum mechanics typically present an *operational* rather than a *mechanical* derivation of the Stern-Gerlach phenomenology. Trajectories do not appear. The Stern-Gerlach result is often *postulated* rather than *derived* from the microscopic dynamics, often serving to illustrate or motivate the axioms of standard quantum mechanics. In the present paper, we have given a detailed visualisation of electron trajectories encountering an inhomogeneous magnetic field. No ambiguity remains on what is meant by “measuring spin”, or by the “collapse” of the wave function.

Moreover, we have demonstrated the mechanics of spin-entanglement by visualizing the trajectories of an EPR-pair, showing how the Stern-Gerlach measurement of one electron also affects the motion of the other, determining the possible outcomes in the case of a spin measurement for this other particle.

Celebrating the centennial of the Stern-Gerlach experiment is obviously a tribute to the original discoverers Otto Stern and Walther Gerlach, who, first by nonbelieving and by misinterpretation, actually came to exhibit a major foundation of Nature’s working on the subatomic scale. It became a cornerstone of modern quantum mechanics. However, we are especially happy to dedicate this paper to the memory of Detlef Dürr, who by insisting on clarity and the importance of a mechanical picture, has encouraged many of us to maintain a Boltzmannian perspective in terms of particle trajectories in the modeling and study of quantum matter as well [3, 41, 42]:

“We should deny ourselves from any picture of reality.” But are man’s thoughts something different from these images? It is only God of whom we must not and cannot make any picture.

— Boltzmann’s first answer to the *energeticists*, in: *A word from mathematics on energetics*, Populäre Schriften, Barth, Leipzig (1905) [43].

Acknowledgment: WS acknowledges support from the Research Foundation Flanders (Fonds Wetenschappelijk Onderzoek, FWO), Grant No. G0C3322N, and thanks Siddhant Das for discussions.

References

- [1] D. Bohm and B. Hiley, *The Undivided Universe: An Ontological Interpretation of Quantum Theory* (Routledge, 1993).
- [2] P. Holland, *The Quantum Theory of Motion* (Cambridge University Press, Cambridge, 1993).
- [3] D. Dürr and S. Teufel, *Bohmian Mechanics* (Springer-Verlag, 2009).
- [4] D. Dürr, S. Goldstein, R. Tumulka, and N. Zanghì, “Trajectories and particle creation and annihilation in quantum field theory”, *J. Phys. A* **36**, 4143–4149 (2003).
- [5] D. Dürr, S. Goldstein, R. Tumulka, and N. Zanghì, “Quantum Hamiltonians and Stochastic Jumps”, *Commun. Math. Phys.* **254**, 129–166 (2005).
- [6] D. Dürr, S. Goldstein, R. Tumulka, and N. Zanghì, “Bohmian Mechanics and Quantum Field Theory”, *Phys. Rev. Lett.* **93**, 090402 (2004).
- [7] D. Dürr, S. Goldstein, R. Tumulka, and N. Zanghì, “Bell-type quantum field theories”, *J. Phys. A* **38**, R1–R43 (2005).
- [8] S. Colin and H. Wiseman, “The zig-zag road to reality”, *J. Phys. A* **44**, 345304 (2011).
- [9] W. Struyve, “On the zig-zag pilot-wave approach for fermions”, *J Phys Math. Theor.* **45**, 195307 (2012).
- [10] R. Penrose, *The Road to Reality: A Complete Guide to the Laws of the Universe* (Jonathan Cape, London, 2004).
- [11] M. J. Schnitzer, “Theory of continuum random walks and application to chemotaxis”, *Phys. Rev. E* **48**, 2553–2568 (1993).
- [12] A. E. Patteson, A. Gopinath, M. Goulian, and P. E. Arratia, “Running and tumbling with E. coli in polymeric solutions”, *Sci. Rep.* **5**, 15761 (2015).
- [13] C. Maes, K. Meerts, and W. Struyve, “Diffraction and interference with run-and-tumble particles”, *Phys. A: Stat. Mech. Appl.* **598**, 127323 (2022).

- [14] J. S. Bell, *Speakable and Unspeakable in Quantum Mechanics* (Cambridge University Press, 1987).
- [15] C. Philippidis, C. Dewdney, and B. Hiley, “Quantum interference and the quantum potential”, *Il Nuovo Cimento* **52**, 15–28 (1979).
- [16] P. Holland and C. Philippidis, “Implications of Lorentz covariance for the guidance equation in two-slit quantum interference”, *Phys. Rev. A* **67**, 062105 (2003).
- [17] M. Gondran and A. Gondran, “Numerical simulation of the double slit interference with ultracold atoms”, *Am. J. Phys.* **73**, 507–515 (2005).
- [18] W. Gerlach and O. Stern, “Der experimentelle Nachweis der Richtungsquantelung im Magnetfeld”, *Z. Für Phys.* **9**, 349–352 (1922).
- [19] W. Pauli, “Über den Zusammenhang des Abschlusses der Elektronengruppen im Atom mit der Komplexstruktur der Spektren”, *Z. Für Phys.* **31**, 765–783 (1925).
- [20] G. E. Uhlenbeck and S. Goudsmit, “Ersetzung der Hypothese vom unmechanischen Zwang durch eine Forderung bezüglich des inneren Verhaltens jedes einzelnen Elektrons”, *Naturwissenschaften* **13**, 953–954 (1925).
- [21] G. E. Uhlenbeck and S. Goudsmit, “Spinning Electrons and the Structure of Spectra”, *Nature* **117**, 264–265 (1926).
- [22] A. Pais, “George Uhlenbeck and the discovery of electron spin”, *Phys. Today* **42**, 34–40 (1989).
- [23] C. Maes, *Facts of Matter and Light: Ten Physics Experiments that Shaped Our Understanding of Nature* (Springer International Publishing, Cham, 2023).
- [24] C. Dewdney, P. Holland, and A. Kyprianidis, “What happens in a spin measurement?”, *Phys. Lett. A* **119**, 259–267 (1986).
- [25] C. Dewdney, P. Holland, and A. Kyprianidis, “A quantum potential approach to spin superposition in neutron interferometry”, *Phys. Lett. A* **121**, 105–110 (1987).
- [26] C. Dewdney, P. R. Holland, and A. Kyprianidis, “A causal account of non-local Einstein-Podolsky-Rosen spin correlations”, *J. Phys. Math. Gen.* **20**, 4717 (1987).
- [27] C. Dewdney, P. R. Holland, A. Kyprianidis, and J. P. Vigièr, “Spin and non-locality in quantum mechanics”, *Nature* **336**, 536–544 (1988).
- [28] M. Gondran and A. Gondran, “Measurement in the de Broglie-Bohm interpretation: Double-slit, Stern-Gerlach, and EPR-B”, *Phys. Res. Int.* **2014**, 1–16 (2014).
- [29] T. Norsen, “The pilot-wave perspective on spin”, *Am. J. Phys.* **82**, 337–348 (2014).
- [30] J. Bricmont, *Making sense of quantum mechanics* (Springer International Publishing, 2016).
- [31] R. Tumulka, *Foundations of Quantum Mechanics*, Lecture Notes in Physics (Springer International Publishing, 2022).
- [32] D. Dürr, S. Goldstein, and N. Zanghì, “Quantum Equilibrium and the Origin of Absolute Uncertainty”, *J. Stat. Phys.* **67**, 843–907 (1992).
- [33] C. Colijn and E. Vrsçay, “Spin-dependent Bohm trajectories for hydrogen eigenstates”, *Phys. Lett. A* **300**, 334–340 (2002).
- [34] A. Einstein, “Elementare Überlegungen zur Interpretation der Grundlagen der Quanten-Mechanik”, in *Scientific Papers Presented to Max Born: On His Retirement from the Tait Chair of Natural Philosophy in the University of Edinburgh* (Oliver and Boyd, 1953), pp. 33–40.

- [35] W. C. Myrvold, “On some early objections to Bohm’s theory”, *Int. Stud. Philos. Sci.* **17**, 7–24 (2003).
- [36] A. Böhm, *Quantum Mechanics: Foundations and Applications*, 2nd ed. (Springer, New York, 1986).
- [37] B. C. Hsu, M. Berrondo, and J.-F. S. Van Huele, “Stern-Gerlach dynamics with quantum propagators”, *Phys. Rev. A* **83**, 012109 (2011).
- [38] K. Meerts, *Zig-zag electrons*, <https://github.com/kaspermeerts/zigzagelectrons>, 2023.
- [39] D. Dürr, S. Goldstein, R. Tumulka, and N. Zanghì, “On the Role of Density Matrices in Bohmian Mechanics”, *Found. Phys.* **35**, 449–467 (2005).
- [40] D. Z. Albert, *Time and Chance* (Harvard University Press, 2000).
- [41] D. Dürr, *Bohmse Mechanik als Grundlage der Quantenmechanik* (Springer-Verlag, 1999).
- [42] D. Dürr, S. Goldstein, and N. Zanghì, *Quantum Physics Without Quantum Philosophy* (Springer-Verlag, 2012).
- [43] C. Cercignani, *Ludwig Boltzmann: The Man Who Trusted Atoms* (Oxford University Press, Oxford; New York, 1998).